Looking into a laser textured piston ring-liner contact

Sorin-Cristian Vlădescu[a], Alessandra Ciniero[a], Khizer Tufail[b], Arup Gangopadhyay[c], Tom Reddyhoff[a]

[a] Tribology Group, Department of Mechanical Engineering, Imperial College London, South Kensington, Exhibition Road, SW7 2AZ, London, United Kingdom

[b] Ford Motor Company, Dunton, Essex, United Kingdom

[c] Ford Motor Company, Dearborn, Michigan, United States of America

Abstract

This paper presents an experimental study into the flow behaviour of lubricant in a reciprocating contact simulating a piston ring–cylinder liner pair. The aim was to understand the effects of cavitation, starvation and surface texture, as well as the interaction between these, in order to improve automotive engine performance. A custom-built test rig was used, in which a section of piston ring is loaded against a reciprocating, laser-textured, fused silica pad representing the liner. A fluorescence microscope focusses through the silica specimen onto the contact in order to image the distribution of dyed oil. Tests were performed using a range of texture geometries and orientations, under starved and fully-flooded lubrication conditions, with measurements being compared against those from a non-textured reference.

Under limited oil supply conditions, the non-textured reciprocating contact sweeps oil towards the reversal points (TDC and BDC), leading to starvation and increased friction. This issue is alleviated by the presence of surface texturing, with each pocket transferring oil from the inlet to the outlet of the contact as it passes; the result being 33% lower friction and oil distributed evenly over the liner surface. Even under fully flooded conditions, starvation is shown to occur following each reversal, as the change in sliding direction causes the cavitated outlet to become the oil-deprived inlet. This proof of cavitation-reversal-starvation, which occurs for up to the first 5% of the stroke length, depending on the lubricant's viscosity, corresponds to regions of high wear, measured in this study and on actual cylinder liners reported in the literature. This process is also counteracted by the presence of surface texture, with each pocket depositing oil into the cavitated region prior to reversal.

Fluorescence data also provides insights into other mechanisms with which different textures geometries control friction. Longitudinally oriented pockets increase friction as they appear to connect the high pressure inlet with the low pressure outlet, leading to oil film collapse. Transverse texture produce localised cavitation inside each pocket, which supports the theory that texture draws lubricant into the contact through the 'inlet suction' mechanism.

These findings can aid texture design by showing how pockets can be used in practice to simultaneously control oil consumption, and reduce friction and wear along the stroke.

Keywords: Laser surface texture, Cavitation, Piston rings, Starvation, Friction reduction.

1. Background

1.1 Piston ring-liner lubrication

This research is concerned with understanding and improving the performance of automotive piston-cylinder liner contacts through the application of surface texturing. This contact serves four main functions; to *i*) make a dynamic seal between the combustion chamber and crankcase, *ii*) facilitate heat transfer from the ring to the liner, *iii*) produce a low friction sliding interface and iv) regulate the distribution of oil over the liner.

The main issues associated with piston ring performance that impact engine emissions are blow-by, oil consumption and friction.

Blow-by – *i.e.* the flow of combustion gases past ring-pack into the crankcase – reduces the pressure applied to the piston crown on the power stroke and therefore decreases the work done on rotating the crankshaft. Another undesirable effect of blow-by is that contaminant combustion products are introduced into the oil, which inhibit its effectiveness as a lubricant.

Oil consumption occurs due to oil flow between the crankcase and combustion chamber. This is undesirable since the loss of oil in the engine reservoir must be replaced, which costs money, while the increase in unburnt hydrocarbon exhaust emissions as the oils are vaporised and passed into the exhaust flow. Reducing oil consumption is also important to reduce oil in the exhaust gas that would otherwise clog the particulate filter and poison the catalytic converter [1].

Friction at the sliding piston ring interface consumes work directly from the thermodynamic cycle, and hence reduces the output work and efficiency of the engine. The amount of frictional dissipation depends on the sliding speed and lubrication regime that the contact is operating under. The latter is determined by the lubricant thickness, which in turn depends on the contact force, surface roughness and relative velocity between the piston ring and liner. However, other factors such as wear, starvation (*i.e.* the inadequate replenishment of lubricant caused by the multiple ring contacts and rapid reciprocating motion [2]), and presence of surface texturing also affect friction. It is important to reduce piston-liner friction since it is responsible for wasting a significant portion (~5% [3]) of a vehicle's total automotive fuel energy.

Modifying surface topography is a way of controlling *both* oil consumption and friction. However, few studies have looked at these two effects simultaneously (*i.e.* either surface topography's effect on oil consumption [4,5] *or* friction [6–11] have been studied). Their simultaneous investigation is necessary, since they are clearly interlinked.

1.2 Surface texture

Applying texture – *i.e.* features such as dimples or pockets – to the surface of engineering components is an obvious way to modify friction and has been investigated since the 1960s [12]. Surface texture is particularly suited to reducing friction in piston-liner type contacts, since the relatively low contact pressures preclude stress concentration and fatigue issues, which arise in components involving counter-formal contact such as gears. The impact of this approach can be significant, with friction reductions of over 50% being demonstrated in laboratory controlled tests [13], and some evidence suggests that this translates to measurable improvements in overall engine performance [14]. Compared to other energy saving solutions, surface texture is relatively cheap and simple to implement. It does not require components to be redesigned and can be incorporated easily into existing and future technologies. These reasons have led to an exponential increase in the number of technical publications of the subject, as noticed by Gropper and Wang [15].

The most widespread means of creating surface patterns in engineering components has been Laser Surface Texturing (LST) due to its ability to create micron sized features, using short, often femtosecond, laser pulses. This approach can be applied to a wide range of materials including metals [16], polymers [17], ceramics [18]. However, due to the limitations related to production times and manufacturing costs, other innovative production methods are being explored – these, along with their advantages over LST, have recently been reviewed by Costa and Hutchings [19].

Many of these studies have shown that surface patterns can improve friction, wear and load carrying capacity in fluid film bearings. In the earliest work on micro-texture (1966), Hamilton *et al.* [12] observed that surface texture can improve the load carrying capacity of a mechanical face seal, while later work (1968 - 1969) by Anno *et al.* [20,21] demonstrated a reduction in friction coefficient when using surface texturing. The wear debris entrapment properties of surface texture were later emphasised by Suh *et al.* [22] who concluded in 1994 that the ploughing component of friction in a non-lubricated bearing can be reduced through surface texturing. Following this, major work was later carried out by Etsion and co-workers, as summarised in [23,24].

A number of mechanisms have been suggested to explain how texture can reduce friction, however none have been proved; these include: i) pockets acting as micro-wedge [20] or step bearings [25], ii) pockets increasing the volume of lubricant entrained at the inlet [26], iii) pockets pressurising lubricant due to elastic deformation [27], iv) pockets pressurising lubricant due to cavitation (“inlet suction”) [28,29], v) pockets trapping debris [30], vi) pockets feeding oil into the cavitated region to prevent starvation [13]. In order to apply texture effectively in practice, it is vitally important to understand which combinations of these mechanisms occur and under which conditions.

Recent work at Imperial College [13,31–36] has investigated a variety of surface texture geometries in a contact closely replicating an automotive piston ring-cylinder liner pair. The relationship between the friction reduction capability of surface texture and lubrication regime was characterised in [13] for a variety of textured shapes, while in [35,37] rules for the optimum pocket width, depth and spacing was established for the best performing shape determined previously (*i.e.* rectangular pockets orient normal to the direction of sliding, so as to be completely entrapped inside the contact). To help understand the mechanisms leading to the observed friction reductions of textured surfaces, film thicknesses were measured for the first time in a textured reciprocating contact operating in mixed lubrication regimes [31]. This showed that pockets act to increase the oil film thickness by 10s of nanometres, causing a reduction in asperity contact and hence significant reductions in friction due to the steepness of the Stribeck curve in the mixed regime. The transient behaviour of individual pockets passing through the contact was studied in [32], where it was shown that pocket entrainment frequency is more important than physical spacing between pockets. In the most recent study [33], a close correlation was found between the amount of wear in the vicinity of the reversal point and the volume of oil within the pockets. This current study sheds light on the mechanisms behind these observations, in particular for cavitated and starved reciprocating contacts.

1.3 Cavitation

The phenomenon of cavitation is prevalent around piston ring-liner interfaces due to the converging diverging geometry of the contact and the lubricant's inability to sustain sub-ambient pressures [38], which leads to its transition from a liquid to a gas-liquid mixture. Cavitation manifests itself as gas pockets that form inside the lubricant at the rear or the contact. We suggest that the presence of cavitation is important as it can cause lubricant starvation due to the reciprocating nature of the contact. Fortunately, it has been suggested that such cavitation induced starvation may be alleviated by the supply of oil provided by surface pockets [13].

The first to suggest the film rupture boundary condition was Gümbel (1921) [39], while the multiple cavitated regions were first formulated mathematically by Swift (1931) [40] and Stieber (1933) [41]. Since this first suggestion of film rupture, considerable efforts have been made to investigate cavitation behaviour in various types of bearings, both numerically and experimentally. With regard to the theoretical investigation, a sequence of papers by Jacobson and Floberg [42], Olsson [43] and Floberg [44,45] were published between 1957 and 1974, proposing what is collectively referred to as the JFO theory boundary conditions. This theory was the first attempt at defining the reformation boundary conditions necessary to express closed cavities and the related change in expected load-carrying capacity.

Various experimental contributions to the understanding of film rupture and pressure variation in the cavitated region were made by Dowson *et al.* [46,47] and Etsion and Ludwig [48], both groups relying on photography techniques and pressure measurements. Arcoumanis *et al.* [49,50] have also documented the cavitation pattern variation in reciprocating piston ring-liner assemblies while simultaneously measuring the lubricant film thickness, either by employing capacitance [49] or laser induced fluorescence [50]. Most recently, Tang *et al.* [51] employed a digital holographic microscope to perform measurements of the cavitation bubbles generated in a sliding linear contact replicating the ring-liner pair. They observed closed cavitation streamers when a plane glass was driven by a bi-directional translation stage against a cylindrical lens. Phase maps captured by a CCD (charge-coupled device) camera were processed to reveal thickness measurements of the cavitation bubbles.

Despite these advances, there remains uncertainty and disagreement regarding the nature of cavitation in piston ring-liner contacts. For instance, recently, using a numerical model based on a modified Elrod's cavitation algorithm [52], Chong and Teodorescu [53] found that, although cavitation decreases considerably in close proximity to top dead centre (TDC) and bottom dead centre (BDC), it does not disappear altogether. Chong and Teodorescu [53] also found that *"the 'pre-reversal' cavitation is sealed off by the lubricant and forms a bubble at the inlet. Although this is gradually absorbed by the lubricant film, before it fully vanishes, the inlet is starved"*. This consequently leads to thinner lubricant films and higher friction forces. However, in a more recent study [54], after developing a 1D model to analyse the squeeze film lubrication effects in a reciprocating contact replicating the piston ring-liner pair, Taylor concludes that *"around reversal positions, the whole of the piston ring is covered with oil, and there is no cavitation"*. It is important to resolve this discrepancy, since the presence at reversal of the gas-filled outlet, which then becomes the oil deprived inlet, is clearly problematic and should be remedied.

Another area requiring further investigation regards the interaction between surface texture and the cavitated region. The only experimental study in this area carried out to date, showed that pockets can supply oil to the cavitated region and that this may reduce subsequent starvation [13].

It can be concluded from this introduction that *i)* surface texture is an effective means of reducing piston ring-liner friction, but the mechanisms responsible are not well understood, *ii)* surface texture may also affect the distribution of lubricant on the liner surface and therefore may be used to control oil consumption, *iii)* surface texture may affect cavitation behaviour by causing inlet suction to increase load support and also by bringing oil into the gas filled regions to prevent starvation and hence high friction and wear at TDC and BDC. These three effects are clearly interlinked, but to date only the first one has been studied in any detail. It is the aim of the current research to experimentally investigate these effects by imaging the distribution of oil in a

simulated piston-liner contact, in order to assess the suitability of using surface texturing to improve the overall piston-cylinder performance in internal combustion engines.

2. Test apparatus, specimens and procedure

The custom-built reciprocating rig used for this study is presented in Figure 1. In addition to high resolution friction force recordings, the apparatus described in detail in [13,31,32], allows for film thickness and cavitation pattern to be captured using two high sensitivity optical imaging techniques: *i)* a modified version of the ultrathin film interferometry technique that is able to measure nanometer size film thicknesses in textured reciprocating contacts operating in mixed and boundary regimes, and *ii)* a laser-induced fluorescence (LIF) technique to qualitatively image the distribution of oil in and around the reciprocating ring-liner pairing. The latter technique will be the focus of the present study.

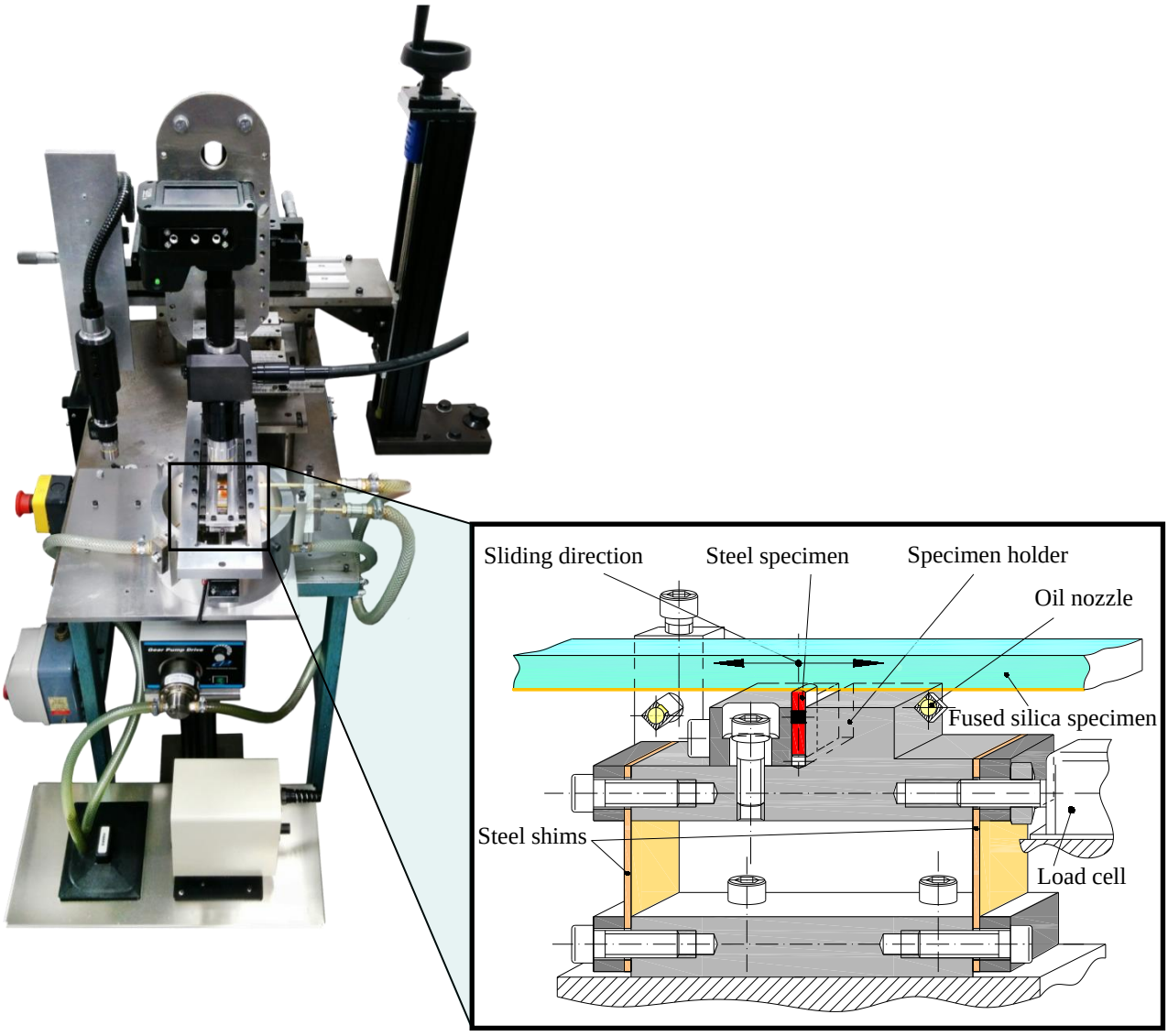

Figure 1 *– Layout of the reciprocating test rig.*

The LIF system set-up is based on the photo-excitation of a fluorescent dye and comprises three main components shown in Figure 2. Due to the high quantity of dye required to blend with the 7 litres of oil required by the rig, the commercially available oil tracer, “Dye-Lite”, was chosen. The light from a Mercury–Xenon source is directed towards a beam splitter, located between the high speed camera and microscope objective. The light enters the beam splitter through an exciter (band pass) filter which limits the transmission of wavelengths to a specified range. The fluorescent light emitted by the excited specimen then passes through a second filter, the emission (long pass) filter, which removes wavelengths below a specified value, before being captured by the camera. The minimum wavelength for the emission filter is selected to ensure that only the light-induced fluorescence from the dye/lubricant mixture is ultimately recorded (Figure 2 – detail).

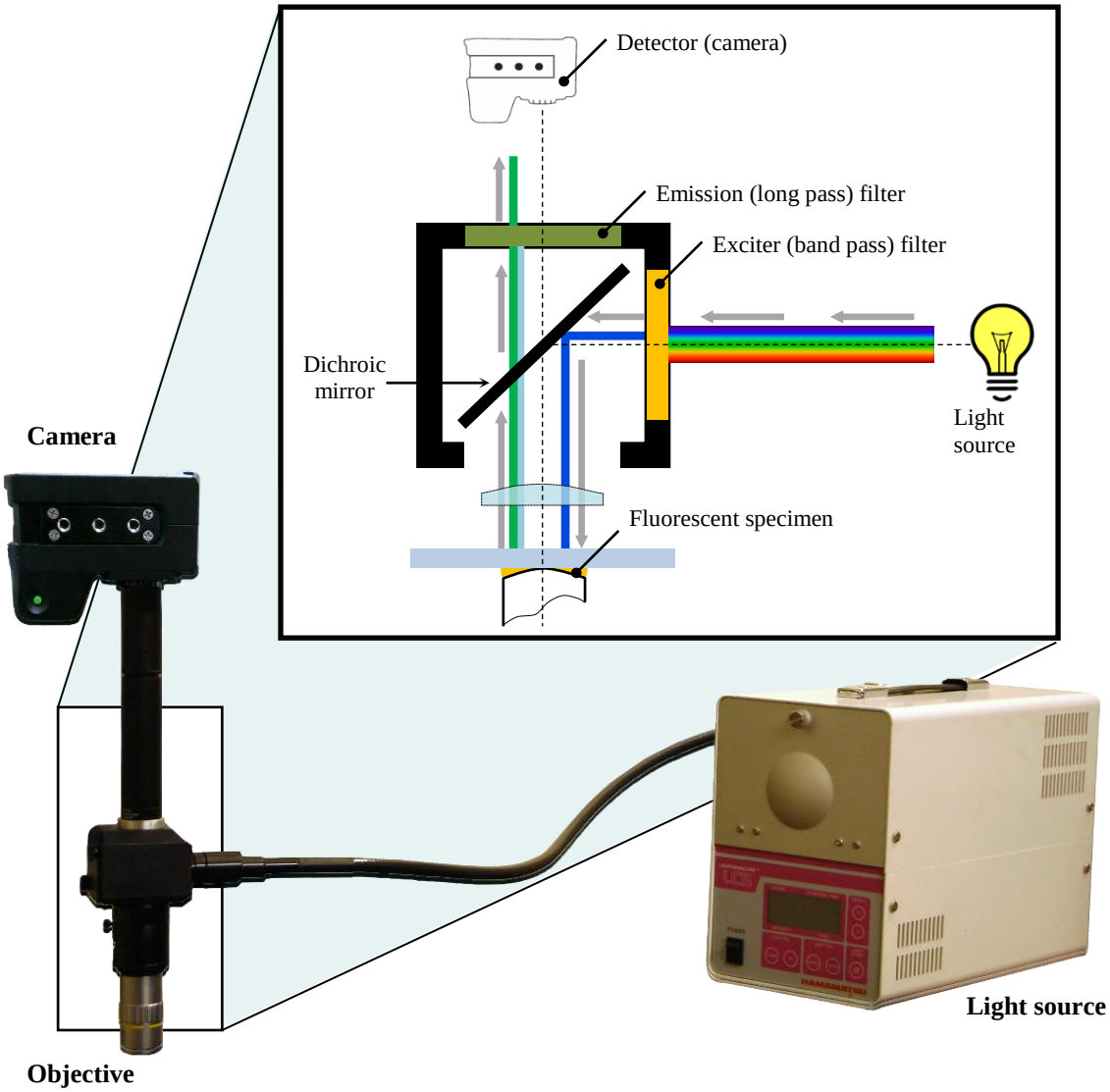

Figure 2 *– Laser Induced Fluorescence (LIF) microscope system; schematic representation of the fluorescent cube and the light path inside the microscope.*

With regard to the mechanical part of the test apparatus, the fused silica plate (replicating the cylinder liner) is driven by an electric motor via an adjustable stroke mechanism (the stroke length used in this study is 28.6 mm); the latter is coupled to a 9 bit rotary position encoder, used to determine and control both the velocity of the shaft and its angular position. The counterpart specimen - a convex steel pad replicating the piston ring (radius R = 40 mm, width D = 2 mm and length L = 10 mm), is fixed on a stationary holder which performs two functions: *i)* it allows the automatic self-alignment of the convergent-divergent steel pad on the fused silica specimen and *ii)* it allows the measurement of the frictional response, as the upper part of the holder deflects away from or towards a high sensitivity load cell generating a voltage differential.

For the fully flooded tests, the lubricant is supplied directly to each side of the contact area by a temperature controlled immersion circulator, a series of pumps, and two nozzles attached to the oil bath. By supplying excess oil at an accurately controlled temperature, this system ensures the contact is fully flooded and hence a repeatable frictional response can be captured.

A triggering system was designed and manufactured in-house to help identify the presence of cavitation phenomena at the moment of reversal, and monitor individual pockets passing through the contact. This electronic circuit enables the high-speed camera used for cavitation visualisation to be triggered with a precision of 0.7 degrees of crankshaft revolution (corresponding to a distance of 111.2 μm along the stroke).

The specimens representing the piston rings were designed and manufactured from AISI 52100 steel and fully hardened at 850 kgf/mm^2 (Figure 3(a)). Before commencing the reciprocating tests, the convergent-divergent sides of the samples were mirror polished to achieve the surface finish ilustrated in Figure 3(b) (the final surface roughness values presented in this Figure exclude the curvature of the sample). These specimens were flat in the direction transverse to sliding, in order to produce a line contact when loaded against the flat silica pads detailed below. As described in Section 2, to ensure the correct loading along the length of the contact, the steel pad was fitted with a self-aligning mechanism. This consisted of a hole through which a 4 mm diameter pin was positioned with a +80μm tolerance resulting in continuous self-adjustment with the counterpart silica specimen.

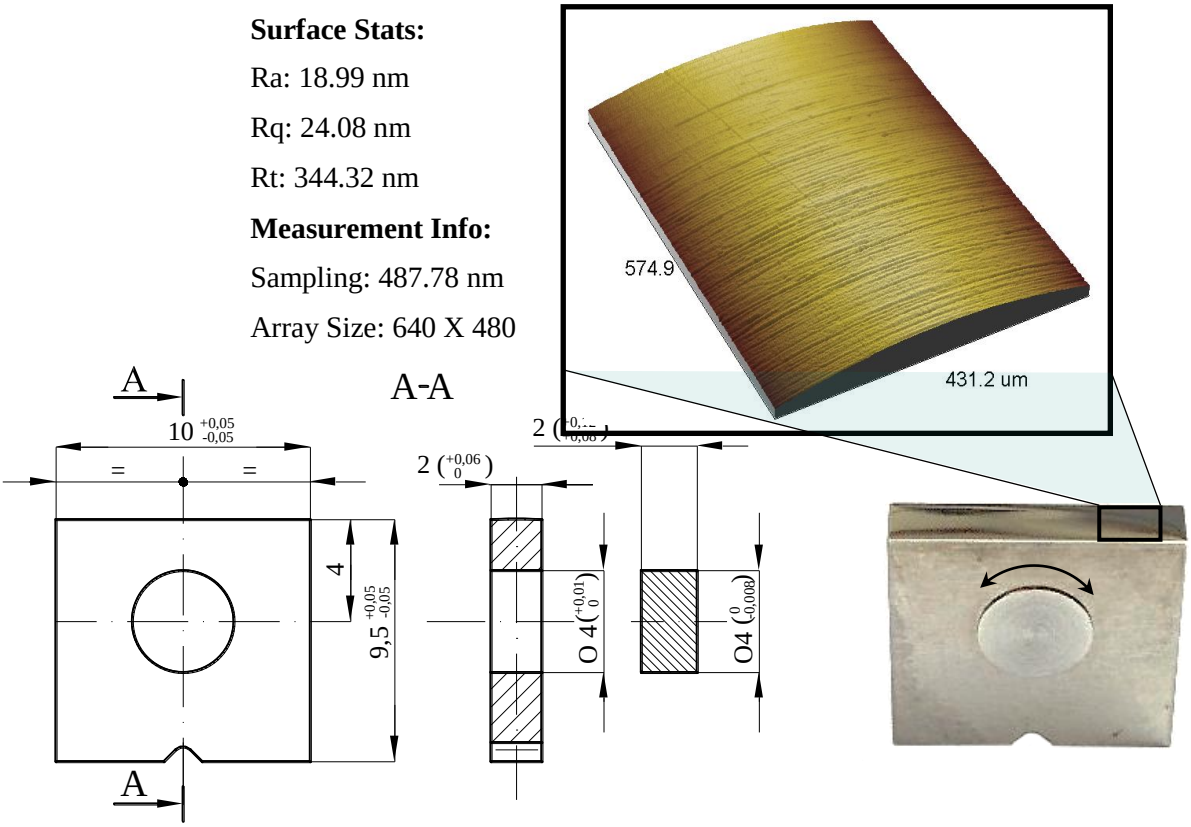

Figure 3 *–Design of the steel specimen allowing self-alignment with the counterpart silica pad; (a) schematic representation; (b) Final pad after the Electrical Discharge Machining together with the three dimensional surface plot of the convex side*

The surface of the counterpart HPFS (high purity fused silica) specimens was laser textured using an ultrafast picosecond laser produced by Oxford Lasers Ltd. At a frequency of 10 kHz, wavelength of 355 nm and power of 5 micro joules, the picosecond laser ensured the ablation of micron-sized portions from the sample surface before the material had time to undergo significant thermal changes. This resulted in a high quality rectangular shape of individual pockets with no piling up of material at the edges of the pocket. The three-dimensional optical profile of the three different textured patterns selected for the curent study are shown in Figure 4, alongside their geometrical and surface parameters.

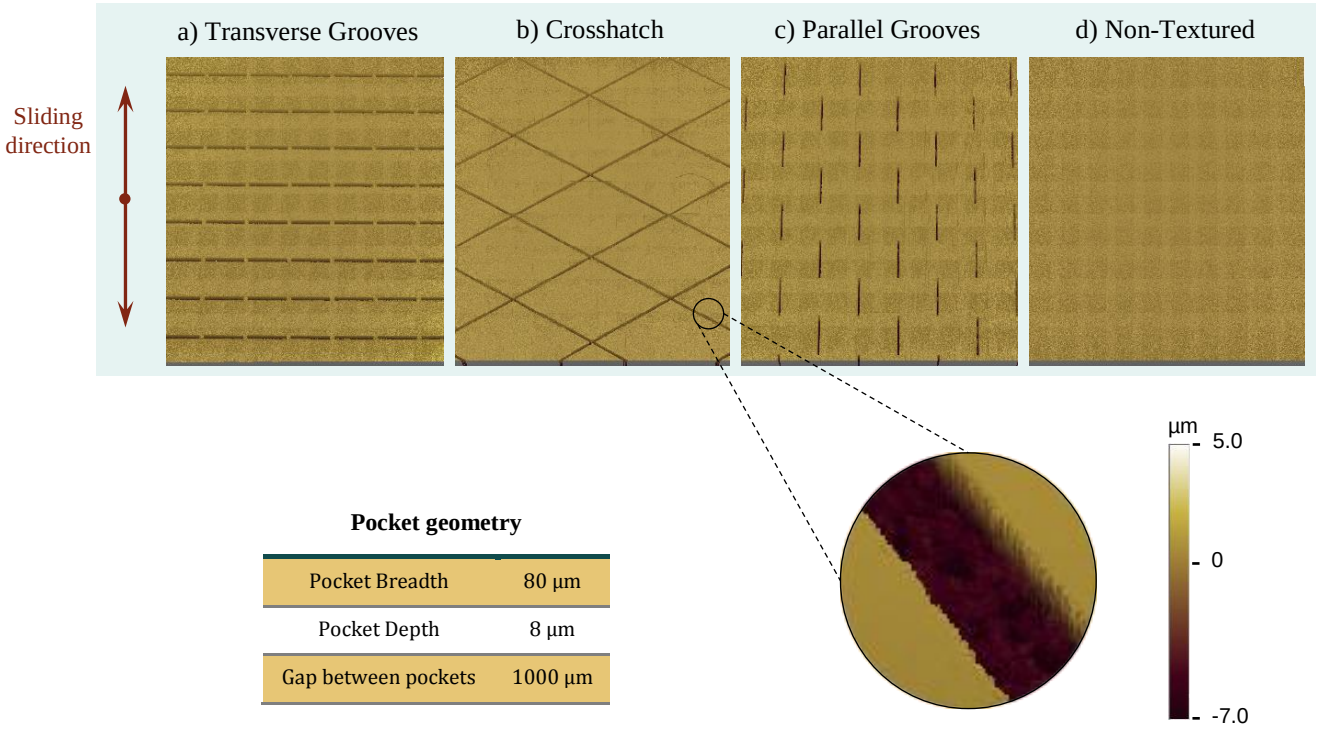

Figure 4 *– Three-dimensional surface plots of fused silica specimens with different textured patterns:(a) Transverse Grooves; (b) Crosshatch; (c) Parallel Grooves; (d) Non-Textured. Images obtained using the Veeco Wyko optical profiler.*

The features making up each pattern had consistent geometries, while pocket depth, breadth and density were maintained constant for an accurate comparison between different shapes. The three textured patterns employed - Transverse Grooves, Parallel Grooves and Crosshatch - were selected based on results from previous findings [13]. Specifically, transverse grooves were selected since this shape, consisting of rectangular features normal to the direction of sliding, which can be completely enclosed inside the contact, gave the greatest friction reductions. Parallel grooves were selected since rectangular features parallel to the direction of sliding were actually shown to increase the frictional response compared to the non-textured reference. Finally, the crosshatch pattern was selected for its close approximation of the plateau honing encountered in IC (internal combustion) engines.

Reciprocating sliding tests were conducted under two different lubrication conditions:

- **Fully flooded** (contact constantly supplied with excess oil) was used when imaging various aspects of cavitation phenomena (*e.g.* reversal-starvation and effect of lubricant viscosity);
- **Starved** (supply of oil to the contact limited to a single 10 µl dose at the beginning of the test) was used when imaging the mechanisms through which surface texture acts to reduce friction force and wear under the conditions encountered in IC engines at the TDC.

Under each condition, tests were performed using both textured and non-textured fused silica specimens. The normal load (applied through a deadweight) and the sliding speed were held constant at 105 N and 2 Hz respectively, throughout the entire testing session.

The lubricant used throughout the study was fully formulated SAE 5W20 engine oil. Its temperature and consequently viscosity were accurately controlled as shown in Table 1. During experiments to study the impact of viscosity on cavitation pattern, the oil temperature was controlled using the setup described in [13].

Table 1 *– Properties of the fully formulated SAE 5W20 engine oil.*

	Oil properties				
Oil Temperature [°C]	**Dynamic viscosity, η [mPa·s]**	**Kinematic viscosity, ν [mm^2/s]**	**Density, ρ [g/cm^3]**	**Load, W [N]**	**Speed, [Hz]**
25	70.46	83.88	0.84	105	2

Friction force stability over time and test repeatability were analysed for both textured and non-textured specimens and confirmed previously in [13,31,32]. Under both mixed/boundary and hydrodynamic lubrication conditions, measurements were shown to be repeatable to within 0.1 N, over a period of months.

3. Results and discussion

Multiple series of reciprocating sliding tests were performed on both textured and non-textured fused silica configurations, producing series of fluorescent images at different crank angles. The same series of tests was performed under both fully-flooded and starved lubrication conditions and for each test, the frictional response was captured simultaneously with the corresponding catalogue of fluorescent images. With the exception of the viscosity dependence tests presented in the Section 4.2, test conditions were kept constant as detailed in Table 1.

4.1 Cavitation at reversal

To assess cavitation at reversal, the lubricant temperature was permanently set at 25°C and tests were performed on a non-textured liner, setting the triggering system to capture a sequence of fluorescent images separated by 1.4 degrees of crankshaft rotation, starting from the moment of reversal (Figure 5). Light blue regions in Figure 5 indicate the presence of oil, while black regions illustrate the cavitation bubbles (lack of oil). In the figure, the sliding direction of the transparent liner specimen, relative to the stationary ring specimen, is indicated. The contact area is schematically represented by the region enclosed by the dotted yellow lines.

Figure 5 shows that, at the moment of reversal (*i.e.* at zero sliding velocity), the cavitated region is clearly evident and is located at the side of the contact that is changing from being the outlet to the

inlet. Following reversal, the first fern cavities are observed after 2.8 degrees of crankshaft rotation (corresponding to a distance of approximately 0.5 mm along the stroke); these fern cavities grow into strings and subsequently streamers as crank angle increases (terms classified in [49]). It should be noted the distance along the stroke associated with the onset of cavitation ferns increases with decreasing lubricant viscosity. Visual proof that the vapour filled cavitated regions are present on both sides of the contact, can be observed in the highlighted image in Figure 5, captured 5.6 degrees of crankshaft revolution after reversal. Furthermore, Figure 5 shows that it is only after approximately 10 degrees of crankshaft revolution (corresponding to approximately 1.6 mm distance in stroke) that the cavitation strings at the contact's inlet disintegrate into bubbles and fully disappear. By this time, according to Dellis and Arcoumanis [49], the pressure inside the bubbles is expected to be atmospheric. One of the main experimental findings of the study is thus that for more than 5% of the stroke length the bearing's inlet is starved, despite the contact being fully flooded with oil. This explains numerous other studies, which have shown localised wear immediately before/after reversal in simulated [33] and actual [55,56] reciprocating piston liner contacts.

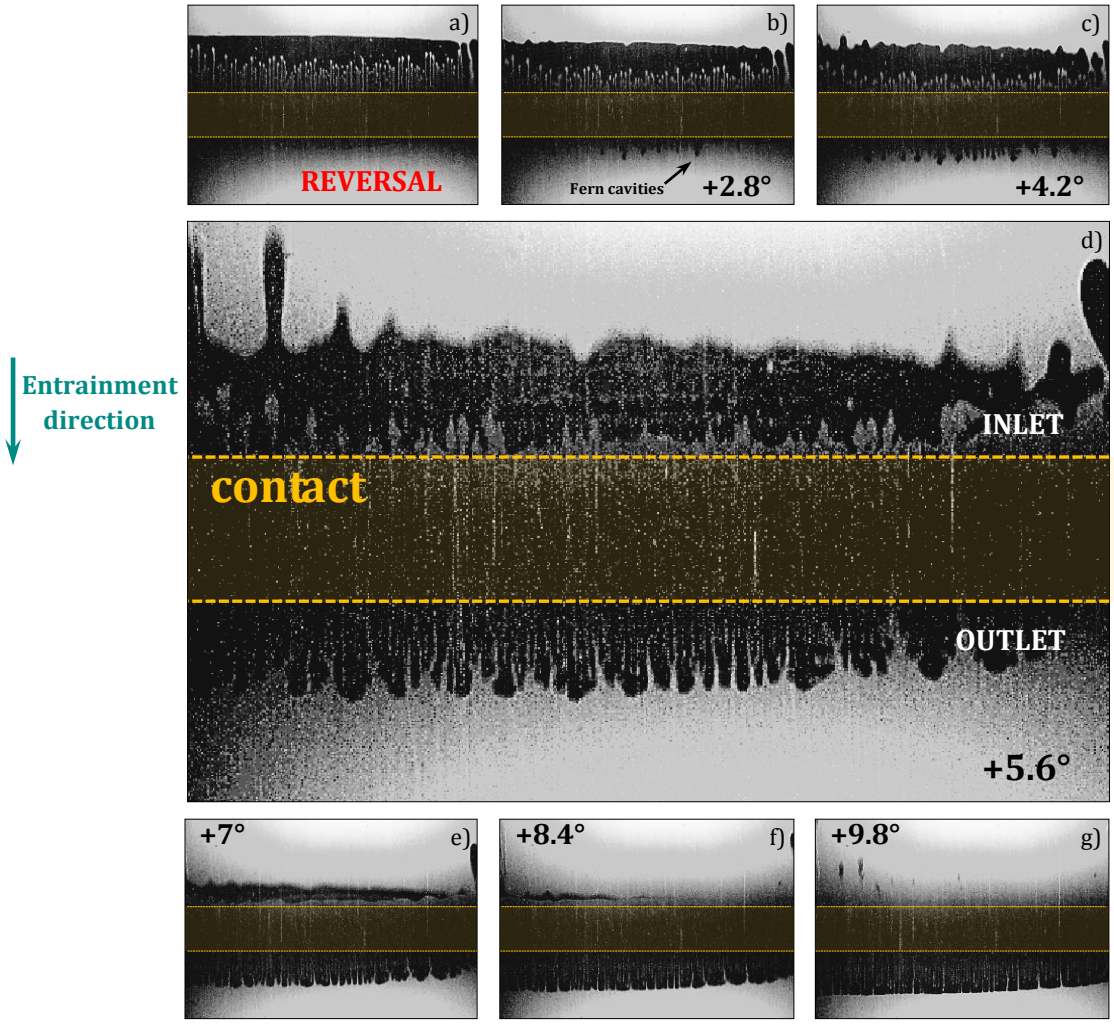

Figure 5 *– Oil distribution captured at intervals of 1.4 degree of crankshaft revolution after the moment of reversal (end of stroke) for a fully flooded non-textured contact.*

4.2 Influence of lubricant viscosity on cavitation pattern

As demonstrated in Section 4.1, the cavitated region leads to starvation after reversal. However, the extent of this issue (*i.e.* the distance along the stroke that is starved) depends on the size of the cavitated region, which in turn varies as a function of viscosity. To characterise this effect, tests were conducted in which the cavitation pattern at the contact's outlet was observed while accurately controlling the lubricant's temperature and consequently viscosity. Here, a non-textured fused silica liner was employed while the oil was continuously supplied to the contact inlet to prevent starvation. The lubricant temperature was controlled between 0°C and 100°C with a temperature stability of 0.2°C using a Thermo Scientific SC150 immersion circulator installed in the test rig oil supply system. The load was kept constant, at a high value of 105 N, which in agreement with findings from [13], justifies the increased number of cavitation striations. With regard to the dependence of the cavitated pattern on temperature, Figure 6 shows a set of five images captured exactly at mid-stroke.

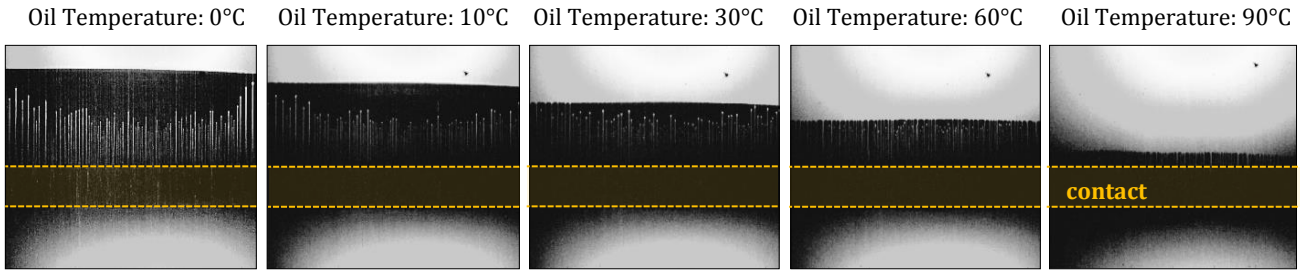

Figure 6 *– Cavitation variation pattern for different oil temperatures; fully flooded non-textured contact.*

It can be observed that, as lubricant temperature increases from 0°C to 90°C, the distance between the contact outlet and the reformation boundary gradually decreases by a factor of five. This implies that cavitation induced starvation at reversal is less severe when the contact is lubricated with a low viscosity oil than a high viscosity oil. For example, when reversal tests were performed after at an oil temperature to 60°C, the bearing's inlet was starved for 1% distance of the stroke length (compared to 6% of the stroke at 25°C).

4.3. Local oil transport and replenishment due to surface texture

To study the impact of surface texture upon starvation and wear, tests were carried out under limited oil supply conditions (only 10 µl of lubricant was applied to the contact before the test), on both textured and non-textured specimens. Figure 7 presents a set of four images captured every 14° crank angle starting from reversal (x), for the non-texture case. Here, it can be observed that the contact inlet is entirely starved following reversal (Figure 7(a)). This is due predominantly to the limited volume of oil being pushed beyond the reversal point, rather than the cavitation induced starvation discovered above. Furthermore it is not until a crank shaft revolution of 42°

that any significant volume of oil has returned to the inlet – eventually doing so by seeping back gradually from the edges of the wear track (indicated by the red arrows in Figure 7d).

This "replenishment" mechanism for the non-textured contact, (put forward more than four decades ago by Chiu [57] who investigating its dependence on lubricant surface tension, viscosity, sliding speed) is severely limited in actual piston liner pairings, due to the continuous line contact with no paths for the oil to flow back to the inlet.

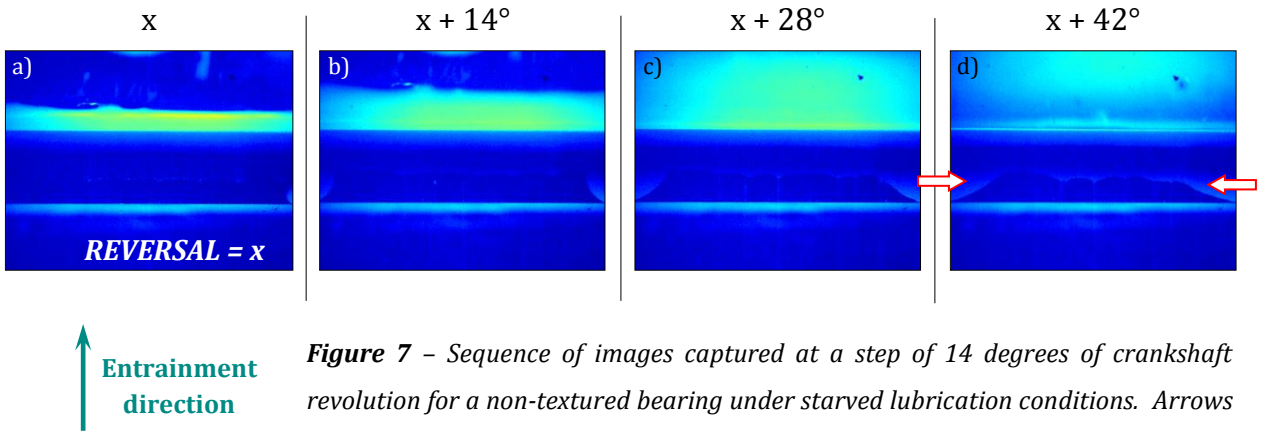

Figure 7 *– Sequence of images captured at a step of 14 degrees of crankshaft revolution for a non-textured bearing under starved lubrication conditions. Arrows indicating lubricant replenishment.*

The behaviour observed in Figure 7 for a non-textured liner was investigated under identical test conditions for a textured specimen (Figure 8). A sequence of fluorescent images was captured at intervals of 7 degrees of crankshaft revolution under starved lubrication conditions. The first image of the sequence, captured at a 21° crank angle before reversal, illustrates the pocket passing through the contact. In the second image, captured at a 14° crank angle before reversal, the pocket is seen leaving the contact, entering the cavitated region, and depositing its oil just outside the contact's outlet. In the third image a second pocket can be observed entering the contact. Then at the moment of reversal, the lubricant deposited by the pocket at the contact's outlet at *x – 14°* is immediately available to flood the new inlet, preventing a starved reversal. In the next three images, the process repeats: the original pocket approaches the contact empty (*x + 7°)*, before being refilled with lubricant available at the inlet (*x + 14°),* and then transports it through the contact (*x + 21°)*.

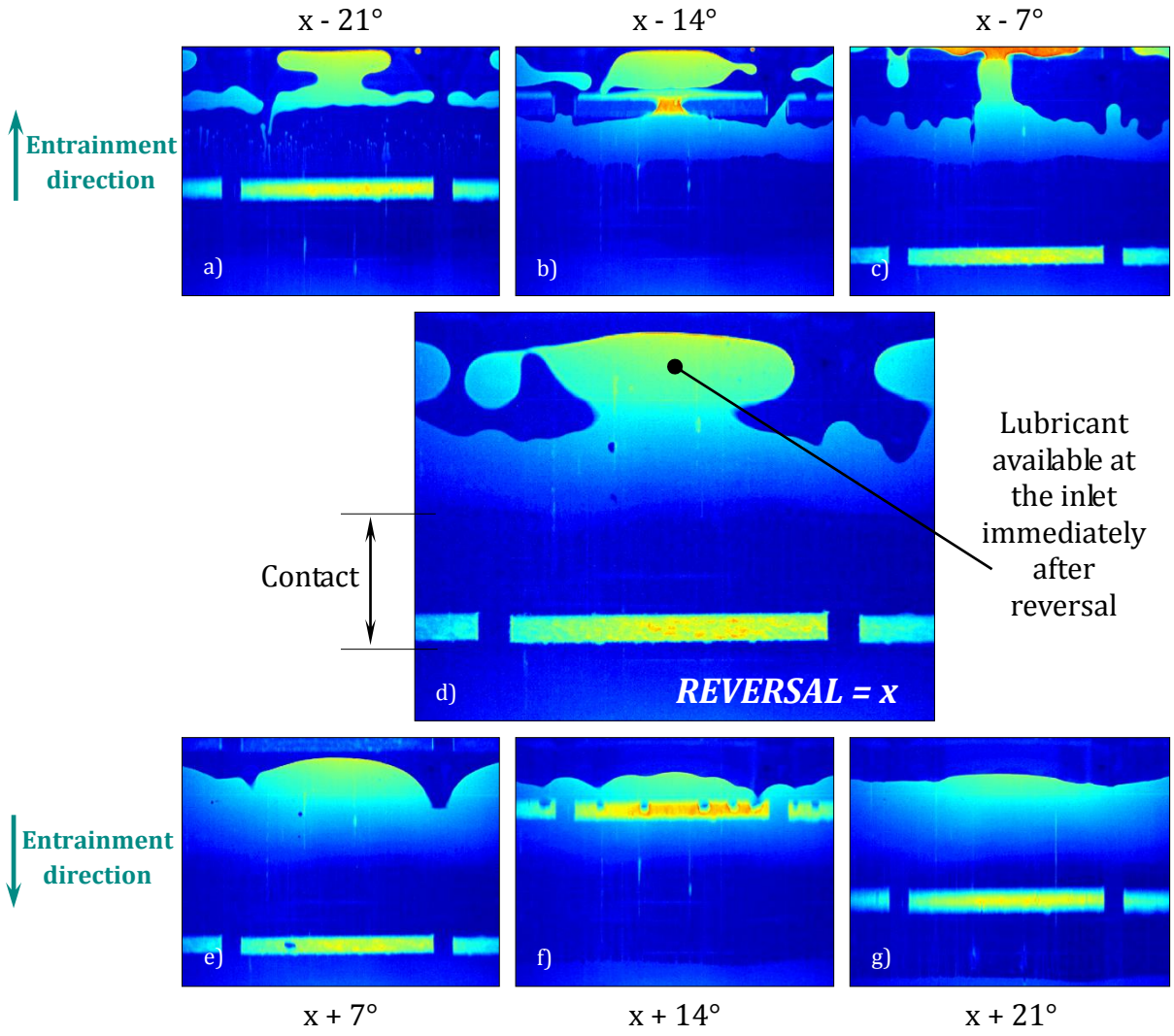

Figure 8 *– Pockets transversal to the direction of sliding passing through contact at a step of 7 degrees of crankshaft revolution.*

The surface texture lubricant transport mechanism described above, is highly beneficial, since it shows that pockets simultaneously perform two important functions in addition to reducing friction: i) they prevent oil from being pushed beyond the reversal points away from the wear track and ii) ensure the contact is fully flooded after reversal. Furthermore, the resulting benefits in terms of wear reduction have already been observed. In a previous study, the authors showed that surface texture reduced wear around reversal and did so in proportion to the volume of the pocket along the stroke [33]. This can be observed by the optical interferometry images of the wear scar close to reversal on the textured and non-textured specimen shown in Figure 9(a) and 9(b) respectively.

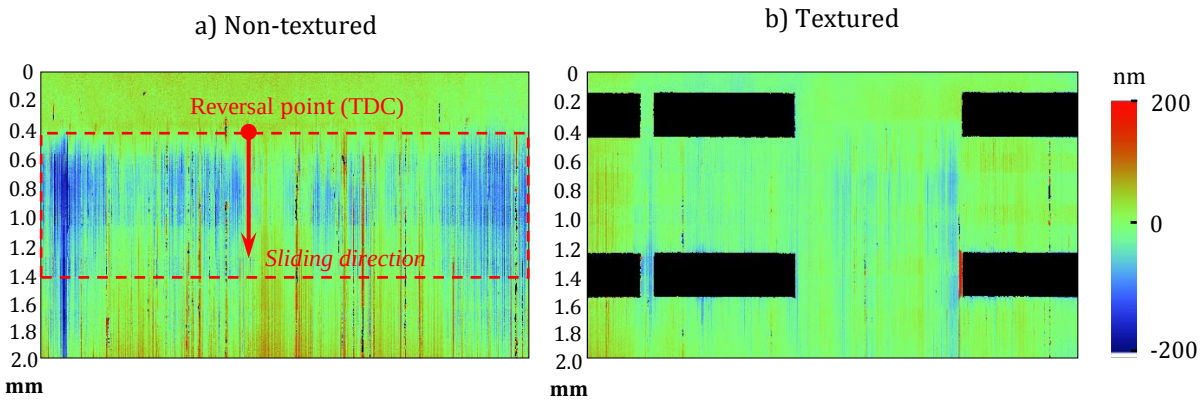

Figure 9 – Wear scar adjacent to reversal for (a) non-textured and (b) textured liner specimen surface [33].

4.4. Overall oil transport and replenishment due to surface texture

A comparison between fully-flooded and starved conditions was performed to assess the impact of surface texture on friction force over a prolonged period of sliding. In these tests, a textured specimen with pockets transverse to the direction of sliding and a non-textured fused silica pad were rubbed against the counterpart steel ring for a period of 60 minutes.

The four possible test combinations were: textured fully-flooded, non-textured fully-flooded, textured starved, non-textured starved. Figure 10 portrays the evolution of the averaged friction force along the stroke (averaged between 30° and 150° crank angle to remove squeeze film effects) for the four arrangements with measurements obtained every 5 minutes. . The “U” shaped variation of the frictional response in the highlighted raw data plots is explained by the contact operating under mixed lubrication conditions (along the stroke, friction decreases with speed due to film formation).

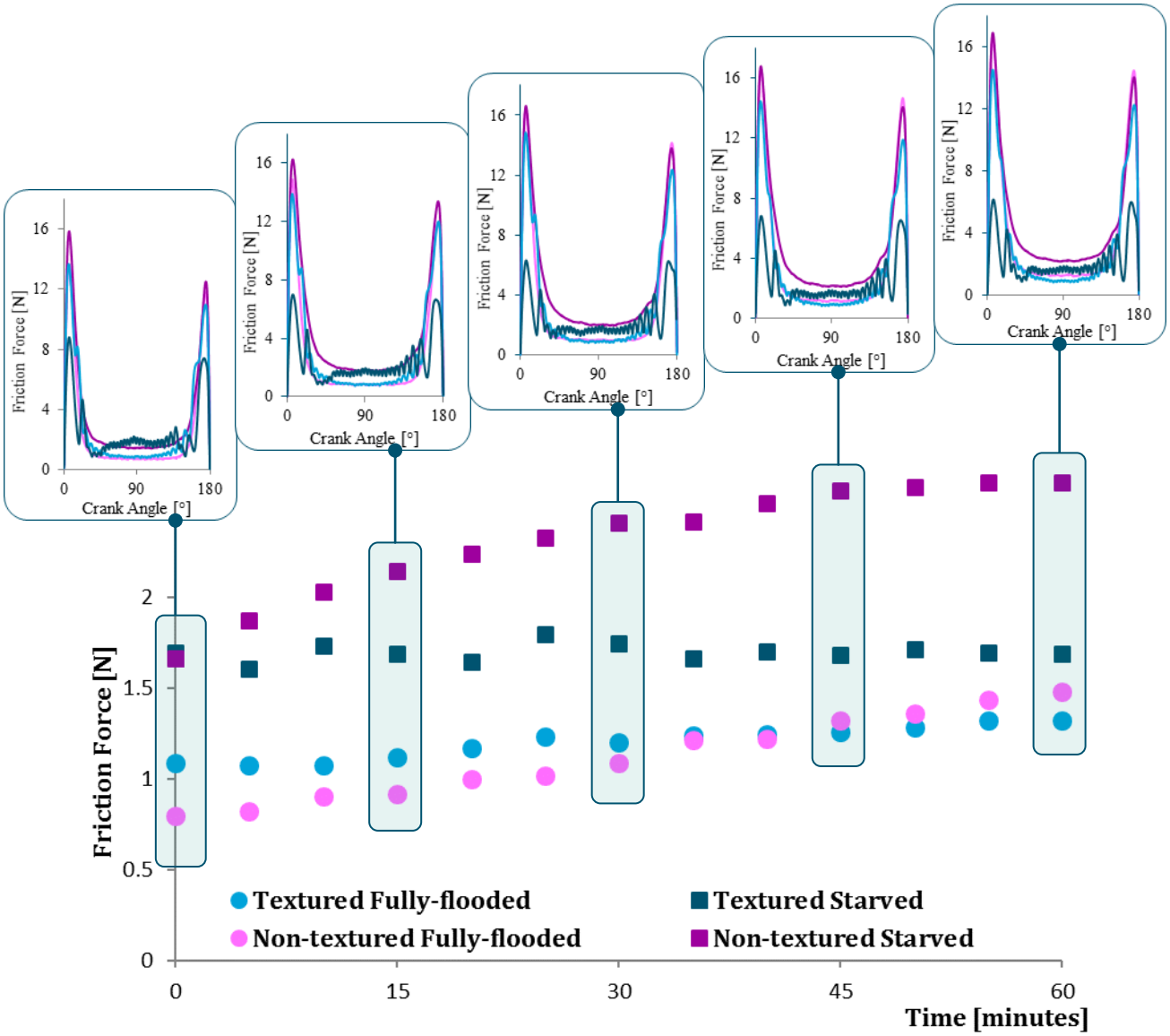

Figure 10 *– Variation of friction with sliding time for both textured and non-textured bearings, under starved and fully-flooded lubrication conditions.*

At the beginning of the test, when the composite roughness of the two surfaces is very low (*i.e.,* 15 nm), the fully-flooded non-textured sample gives the lowest friction; this behaviour is in agreement with previous studies [13,31–33] and is due to the contact operating around the transition between hydrodynamic and mixed lubrication regime. However, as shown in [33], the roughening of the surfaces due to wear causes a transition into the mixed regime where the textured surface begins to outperform the non-textured one (in this case after approximately 40 minutes of rubbing).

With regard to the experiments performed under starved lubrication conditions, often encountered in IC engines around TDC (top dead centre), it can be observed in Figure 10 that the friction force for the non-textured specimen is continuously increasing throughout the entire one hour test. Further inspection of the starved textured combination revealed that friction remains constant during this time. The improved performance of the textured specimen under starved conditions can be explained by the oil transfer mechanisms observed for individual pockets in

Figure 8 - *i.e.* each pocket transfers oil from the inlet to the outlet in order to evenly distribute lubricant along the liner and prevent starvation. To visualise this macroscopic effect, low magnification fluorescent images of the static contact were captured at the end of the test with the ring specimen in the mid-stroke position (Figure 11). In this figure, several unwanted reflections are present, (such as the large circular object, which is caused by a screw head), however despite these, insightful observations can be made.

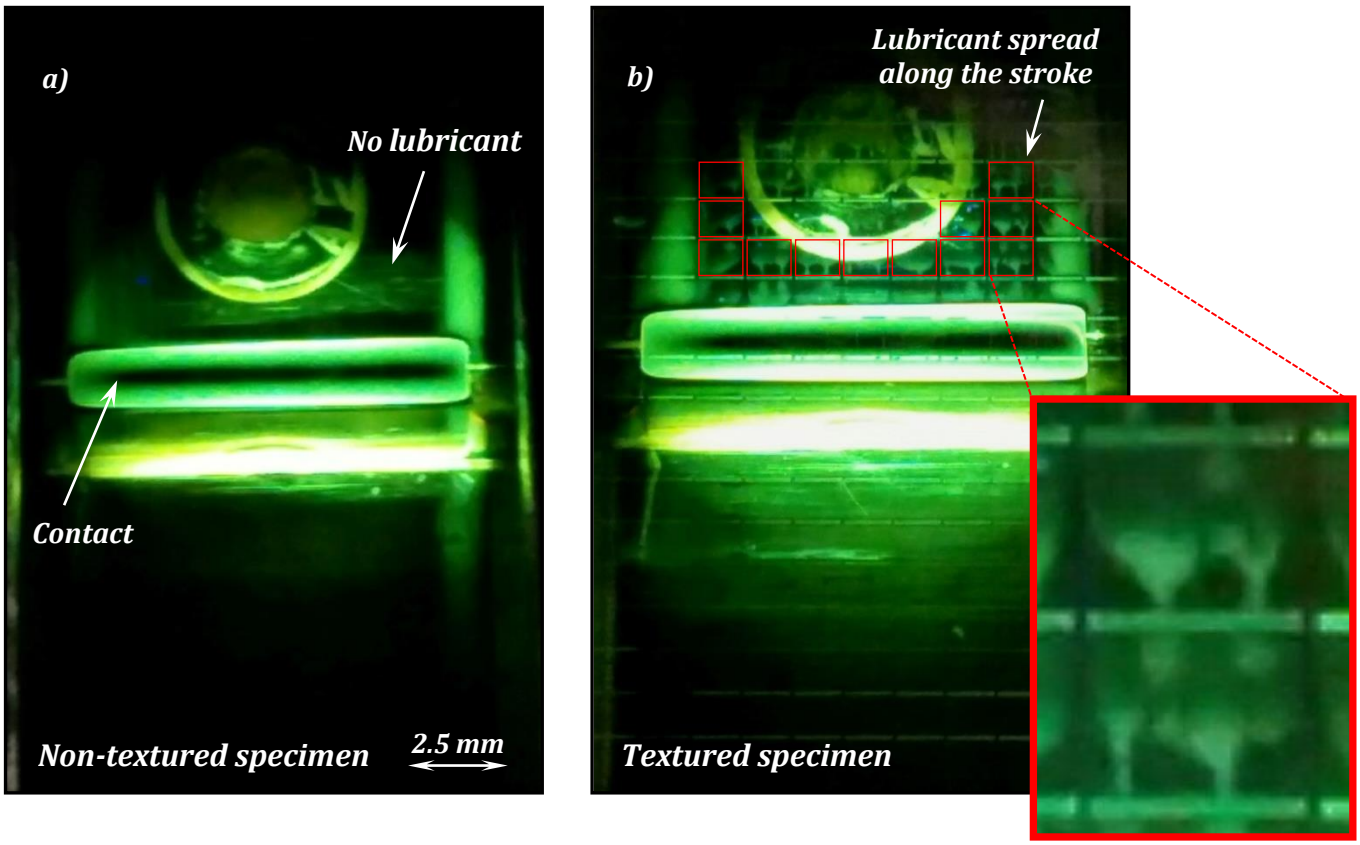

Figure 11 *– Fluorescent images captured at the end of a one hour test for a) a non-textured starved contact and b) textured starved contact.*

After the non-textured test (Figure 11(a)), it can be observed that no lubricant was available for the contact's inlet along the entire length and breadth of the stroke – *i.e.* the contact has pushed the lubricant towards the ends of the stroke in a similar fashion to a windscreen wiper. Conversely, in the textured case (Figure 11(b)), oil is distributed along the entire stroke. This repeatable and uniform spread, observed between any two neighbouring pockets, is clearly visible in the detail of Figure 11. This oil spreading behaviour of surface texture, which occurs throughout the stroke, is a result of the oil-transfer mechanism described in Section 4.2. Note: the oil drops shown in the zoomed inset in Figure 11 correspond exactly to the oil removed from the pocket by the low pressure in the cavitated region and deposited on the liner surface in Figure 8.

This oil transfer behaviour should result in reduced oil consumption in internal combustion engines, since laser produced pockets act to spread the oil along the entire stroke, thus reducing

the burning of lubricant at TDC during the power stroke. Additional studies are however required, employing various pocket geometries and ring radii to optimise this effect.

4.5. Imaging beneficial and detrimental friction effects of pocket shape and orientation

By employing the fluorescence technique under starved lubrication conditions, the final section of this study attempts to assess various texture patterns to understand mechanisms that are responsible for the contrasting friction performances observed in previous studies. It should be noted that the friction controlling reducing mechanisms being investigated in this section occur over the length of the reciprocating stroke (not just around reversal) under fully-flooded conditions [13,31,32] (*i.e.* under conditions of adequate lubricant supply). This means they are separate from the oil transport mechanism described in section 4.2 and 4.3.

As initially observed by Costa and Hutchings [58] and subsequently confirmed by the current authors in [13], pockets orientation relative to the direction of sliding is a critical parameter determining whether the texture pattern has detrimental or beneficial effects on friction. After investigating a range of textured shapes and orientations measuring friction force and film thickness, both studies agreed that grooves parallel to the direction of sliding gave the highest friction force, while grooves perpendicular to the direction of sliding and cross-hatched patterns gave lowest friction.

Figure 12 shows a succession of seven images of a moving pocket under fully flooded conditions, captured using the LIF system; at intervals of 0.7 degree of crankshaft revolution, relative to *x*, which in this case corresponds to the mid-stroke position. It should be noted that this transverse rectangular shaped pocket configuration reduces friction by a significant extent (>50%) compared to a non-textured reference [13,32]. Furthermore, this set of results exposes the appearance of small cavitation bubbles as the pocket exits the contact (x +1.4°). This observation may highlight the occurrence of inlet suction – a previously suggested mechanism by which pockets increase load support [29]. Inlet suction results from the step increase in film thickness seen by the lubricant as it enters the pocket causing a positive normal squeeze and generating cavitation, which locally reduces the pressure and acts to suck additional lubricant into the contact, thus increasing overall load support, which separates the surfaces to reduce friction. This observation is also in agreement with transient friction experiments and numerical modelling focussing on the passage of individual pockets through the contact, carried out by the authors [32]. In that previous study, friction was seen to increase as each pocket entered the contact, (probably due to the reduction in contact area benefiting from hydrodynamic support). This was followed by a rapid decrease in friction, which may correspond to the formation of cavitation bubbles observed in the current study.

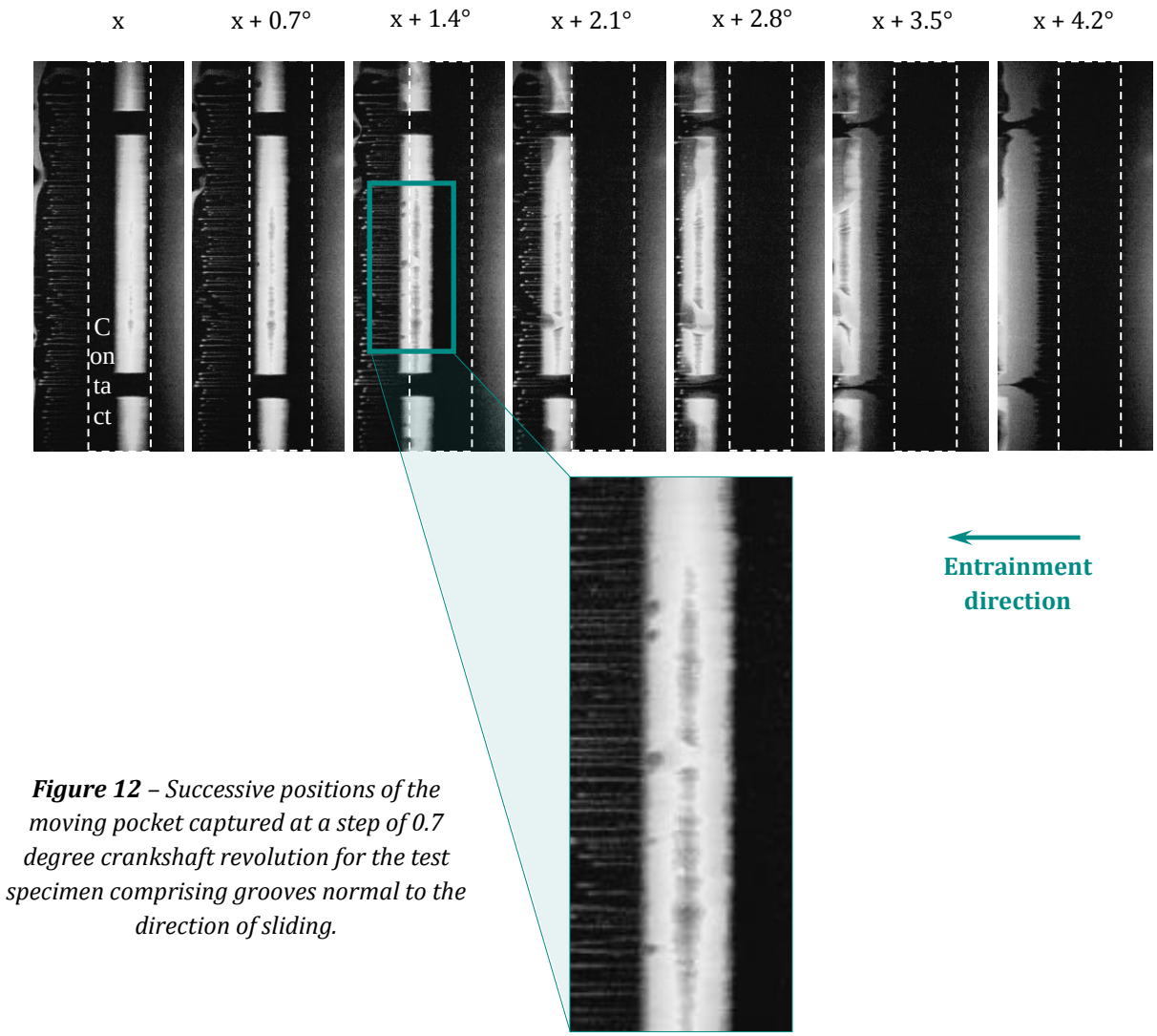

Figure 12 *– Successive positions of the moving pocket captured at a step of 0.7 degree crankshaft revolution for the test specimen comprising grooves normal to the direction of sliding.*

Figure 13 presents a set of fluorescent images captured using a textured pattern comprising pockets orientated parallel to the sliding direction, (which are known to increase friction compared to the non-textured reference [13]). Due to the identical behaviour of each pocket, only the rightmost pocket is discussed. The first image of the sequence, captured at a position *x*° along the stroke, shows the pocket enclosed inside the contact and contains pressurised lubricant, as indicated by its dark red colour. As soon as the leading edge of the pocket leaves the contact and enters the cavitated sub-ambient pressure region at the contact's outlet (Figure 13, *x+1.4°)*, lubricant is immediately drained of the pocket. It is suggested that this occurs because the pocket is effectively forming a pipe between the high pressure inlet and the negative pressure cavitated region and that this oil-suction process collapses the lubricant film causing the high frictional response observed in [13,58].

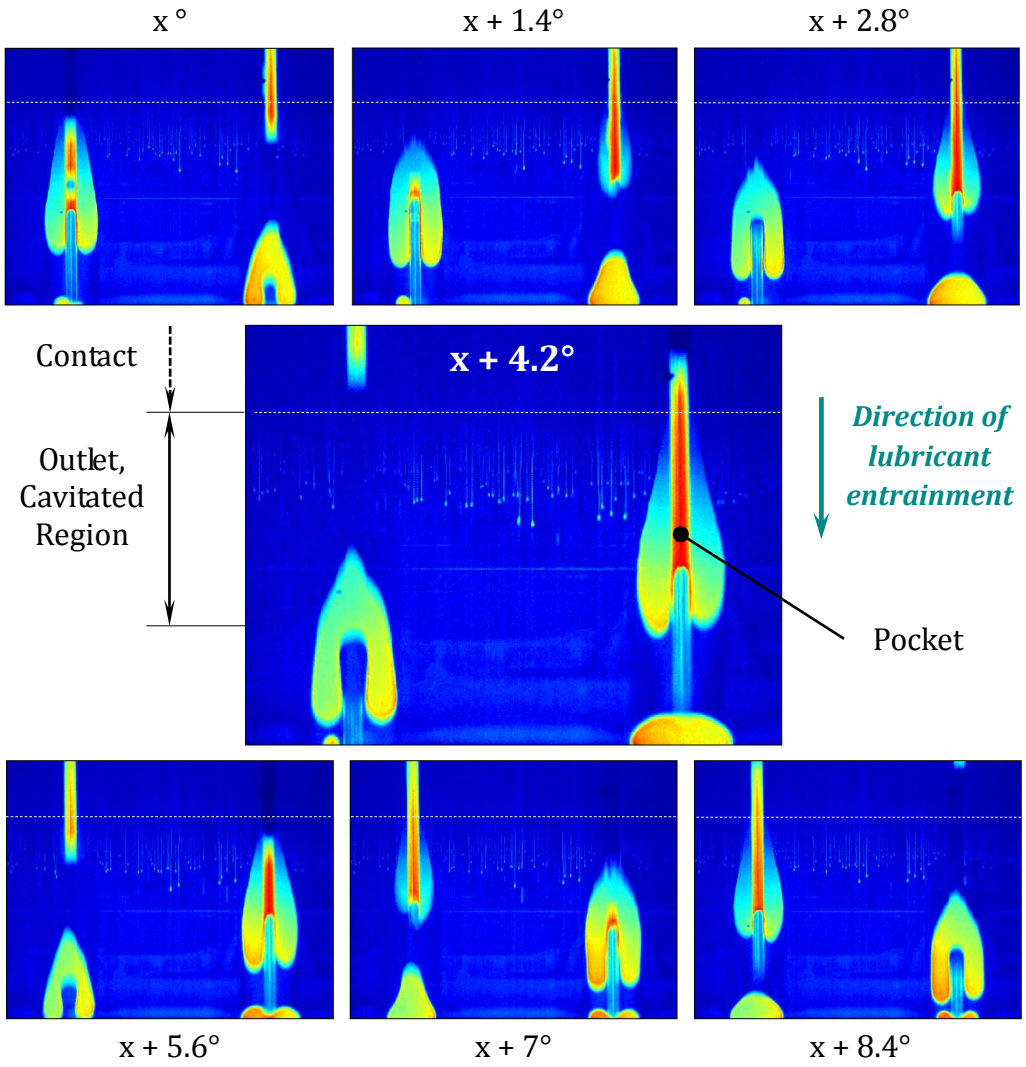

Figure 13 *– Pockets, parallel to the direction of sliding, passing through contact captured at intervals of 1.4 degrees of crankshaft revolution.*

Figure 14 displays the equivalent sequence of images for the crosshatch laser textured pattern. This pattern, in contrast to the parallel grooves, does not appear to suck oil from within the contact, but instead only deposits oil into the cavitated region, *after* the pocket exits the contact area. This can be deduced since the oil leaves the groove and forms a line that is parallel to the line contact in a similar way to the transverse grooves (Figure 14, *x+8.4°)*. The result of this is that the film thickness within the contact is maintained, while at the same time, the lubricant deposited at the outlet both reduces starvation after reversal takes place and ensures an even spread along the stroke. This is again in line with friction data presented in [13], where crosshatch pattern exhibits similar friction reduction to grooves transverse to the direction of sliding. It is interesting to note that the cross hatch geometry, which performs so effectively for the reasons described above, is based on the pattern developed empirically in honing automotive cylinder liners.

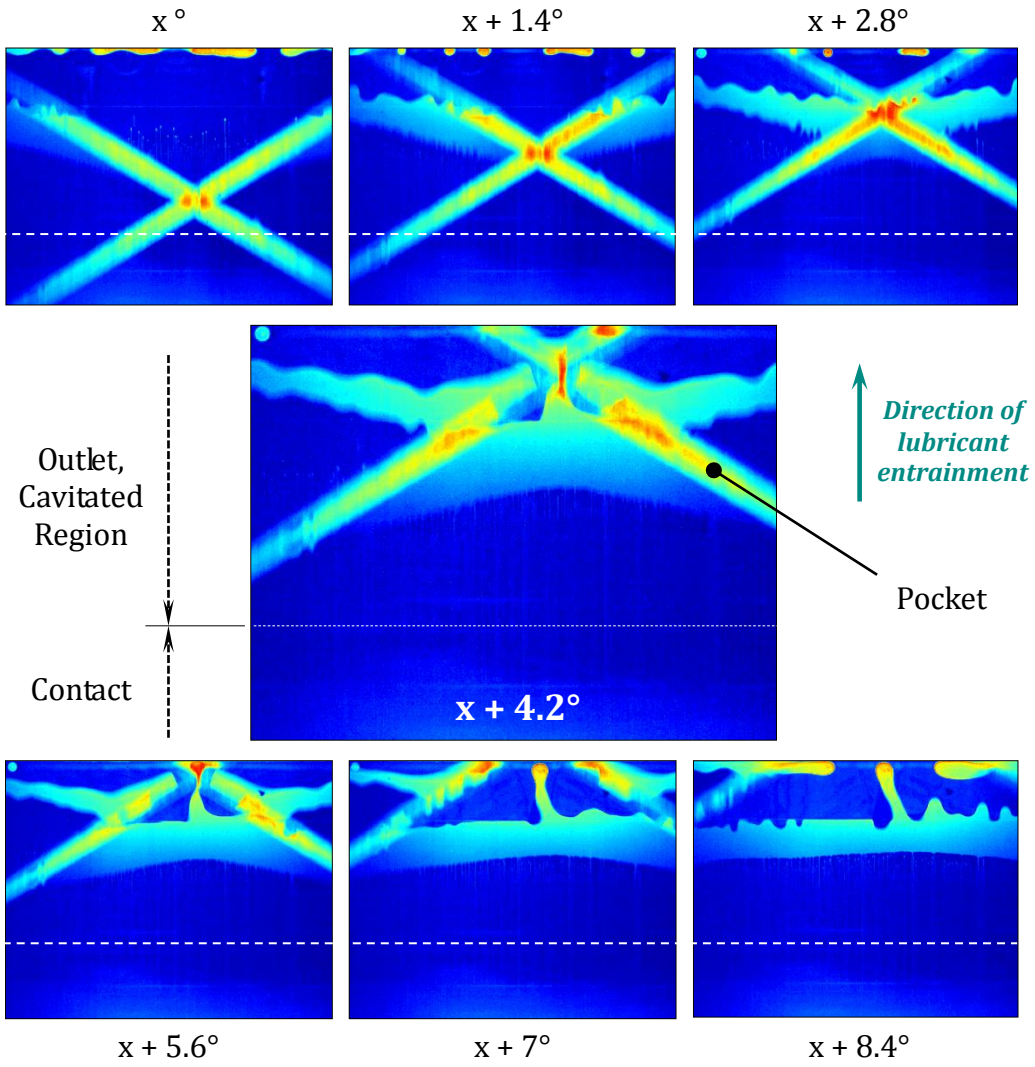

Figure 14 *– Crosshatch laser surface texture passing through contact captured at a step of 1.4 degrees of crankshaft revolution.*

5. Conclusions

A high-speed, laser-induced, fluorescence system coupled to a reciprocating test apparatus representing an automotive piston ring-liner contact was used to investigate the interactions between surface texture and cavitation and the resulting effects on frictional response. This was carried out under starved and fully-flooded lubrication conditions. The friction reduction mechanisms identified can be summarised as follows:

- For non-textured surfaces under conditions of limited oil supply, the finite volume of oil is pushed to the extremities of the wear track by the reciprocating motion of the contact (Figure 15(a)), resulting in increased friction and probably increased oil consumption. This issue is alleviated by the presence of surface texture - *i.e.* as the contact passes, each pocket carries oil from the inlet to the outlet where the reduced pressure in the cavitated region sucks the oil out and deposits it on the liner surface (this mechanism is shown pictorially in Figure 16). The result is an even distribution of oil on the liner specimen,

which would otherwise have been pushed towards BDC and TDC (Figure 15(b)) and friction reductions of up to 33% compared to the non-texture reference.

- Reciprocating contacts experience starvation, even under fully-flooded conditions. This occurs immediately after reversal, when the change in sliding direction causes the cavitated region at the rear of the contact to become the oil deprived inlet. Starved lubrication conditions can then prevail for up to 5% of the stroke length, depending on the lubricant's viscosity (as the viscosity increases, starvation occur for a larger portion of the stroke). This cavitation-reversal-starvation process explains the numerous examples of high wear found close to reversal points in reciprocating contact [33,55,56]. Wear is also alleviated by the presences of surface texture, due to the mechanism in Figure 16 which acts to fill the cavitated region with oil to flood the contact following reversal.

- There is evidence in the literature of surface texture effecting film thickness and friction under fully flooded conditions over the whole length of the stroke (not just around reversal) [31,58]. To gain insights into these effects, which cannot be explained by the lubricant replenishment mechanisms described above, individual entrainments of different pocket geometries were observed. In the case of pockets oriented parallel to the direction of sliding, known to increase friction relative to a non-textured reference [13,58,59], oil could be seen draining out of the contact as the pocket forms a connection between the high pressure inlet and the sub-ambient cavitated region thus collapsing the film. However, during the entrainment of texture oriented transverse to the direction of sliding, cavitation bubbles were observed within each pocket, which supports the mechanism of inlet suction, previously identified by Olver and Fowell [28,29].

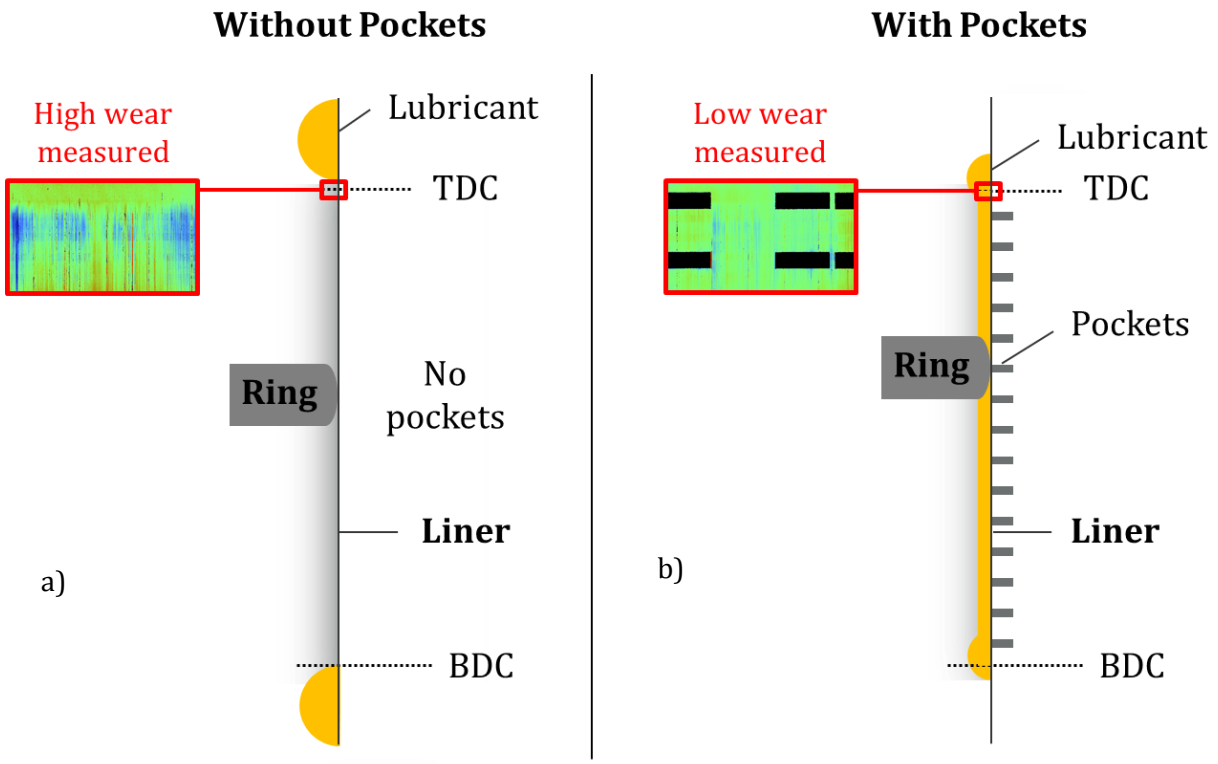

Figure 15 *– Schematic representation of the piston ring - cylinder liner bearing explaining the mechanism of oil transfer along the liner generated by laser surface texture.*

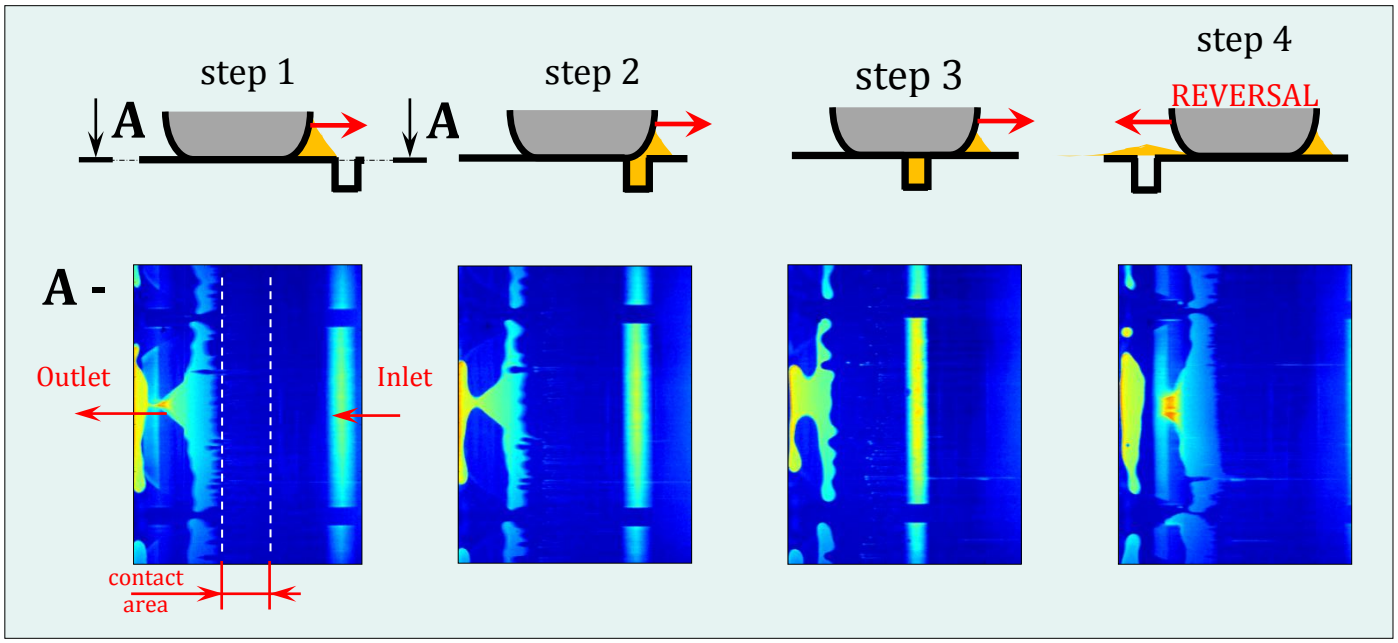

Figure 16 *– Schematic representation of the transient effects of a pocket transverse to the direction of sliding passing through a starved contact. Step 1: partially filled pocket approaches the contact inlet, Step 2: pocket refills with oil from the inlet' meniscus, Step 3: the filled pocket enters the contact (note intensity of dyed oil is greater in Step 1), Step 4: the pocket enters the cavitated region where the sub-ambient pressure sucks oil from and to be deposited on the liner specimen between pockets.*

It can be concluded from this study that the appropriate choice of surface texture pattern is capable not only of reducing piston-cylinder liner friction but also automotive oil consumption.

References

[1] Johansson S, Nilsson PH, Ohlsson R, Anderberg C, Rosén BG. New cylinder liner surfaces for low oil consumption. Tribol Int 2008;41:854–9. doi:10.1016/j.triboint.2008.02.012.

[2] Ma M-T, Sherrington I, Smith EH. Implementation of an algorithm to model the starved lubrication of a piston ring in distorted bores : prediction of oil flow and onset of gas blow-by. Proc Inst Mech Eng , Part J J Eng Tribol 1996;210:29–44. doi:10.1243/PIME.

[3] Holmberg K, Andersson P, Erdemir A. Global energy consumption due to friction in passenger cars. Tribol Int 2012;47:221–34. doi:10.1016/j.triboint.2011.11.022.

[4] Feng C-X, Wang X, Yu Z. Neural networks modeling of honing surface roughness parameters defined by ISO 13565. J Manuf Syst 2002;21:395.

[5] Hill SH, Kantola TC, Brown JR, Hamelink JC. An Experimental Study of the Effect of Cylinder Bore Finish on Engine Oil Consumption 1995. doi:10.4271/950938.

[6] Shen C, Khonsari MM. The Effect of Laser Machined Pockets on the Lubrication of Piston Ring Prototypes. Tribol Int 2016;101:273–83. doi:10.1016/j.triboint.2016.04.009.

[7] Shen C, Khonsari MM. Tribological and Sealing Performance of Laser Pocketed Piston Rings in a Diesel Engine. Tribol Lett 2016;64:26. doi:10.1007/s11249-016-0757-9.

[8] Lu P, Wood R, Gee M, Wang L, Pfleging W. The Friction Reducing Effect of Square-Shaped Surface Textures under Lubricated Line-Contacts—An Experimental Study. Lubricants 2016;4:26. doi:10.3390/lubricants4030026.

[9] Schuh JK, Ewoldt RH. Asymmetric surface textures decrease friction with Newtonian fluids in full film lubricated sliding contact. Tribol Int 2016;97:490–8. doi:10.1016/j.triboint.2016.01.016.

[10] Gu C, Meng X, Xie Y, Yang Y. Effects of surface texturing on ring/liner friction under starved lubrication. Tribol Int 2016;94:591–605. doi:10.1016/j.triboint.2015.10.024.

[11] Usman A, Park CW. Optimizing the tribological performance of textured piston ring-liner contact for reduced frictional losses in SI engine: Warm operating conditions. Tribol Int 2016;99:224–36. doi:10.1016/j.triboint.2016.03.030.
[12] Hamilton DB, Walowit JA, Allen CM. A Theory of Lubrication by Micro- irregularities. Trans ASME J Basic Eng 1966;88:177–85.
[13] Vlădescu S-C, Olver A V., Pegg IG, Reddyhoff T. The effects of surface texture in reciprocating contacts – An experimental study. Tribol Int 2015;82:28–42. doi:10.1016/j.triboint.2014.09.015.
[14] Rahnejat H, Balakrishnan S, King PD, Howell-Smith S. In-Cylinder Friction Reduction Using a Surface Finish Optimization Technique. Proc Inst Mech Eng Part D J Automob Eng 2006;220:1309–18. doi:10.1243/09544070JAUTO282.
[15] Gropper D, Wang L, Harvey TJ. Hydrodynamic lubrication of textured surfaces: A review of modeling techniques and key findings. Tribol Int 2016;94:509–29. doi:10.1016/j.triboint.2015.10.009.
[16] Dumitru G, Romano V, Weber HP, Haefke H, Gerbig Y, Pflüger E. Laser microstructuring of steel surfaces for tribological applications. Appl Phys A Mater Sci Process 2000;70:485–7. doi:10.1007/s003390051073.
[17] Shinkarenko A, Kligerman Y, Etsion I. The effect of elastomer surface texturing in soft elasto-hydrodynamic lubrication. Tribol Lett 2009;36:95–103. doi:10.1007/s11249-009-9464-0.
[18] Zum Gahr KH, Mathieu M, Brylka B. Friction control by surface engineering of ceramic sliding pairs in water. Wear 2007;263:920–9. doi:10.1016/j.wear.2006.11.024.
[19] Costa H, Hutchings I. Some innovative surface texturing techniques for tribological purposes. Proc Inst Mech Eng Part J J Eng Tribol 2014. doi:10.1177/1350650114539936.
[20] Anno JN, Walowit J a., Allen CM. Microasperity Lubrication. J Lubr Technol 1968;90:351–5. doi:10.1115/1.3601568.
[21] Anno JN, Walowit JA, Allen CM. Load support and leakage from microasperity lubricated face seals. Trans ASME J Basic Eng 1969:726–31.
[22] Suh NP, Mosleh M, Howard PS. Control of friction. Wear 1994;175:151–8. doi:10.1016/0043-1648(94)90178-3.
[23] Etsion I. State of the Art in Laser Surface Texturing. J Tribol 2005;127:248. doi:10.1115/1.1828070.
[24] Etsion I. Modeling of surface texturing in hydrodynamic lubrication. Friction 2013;1:195–209. doi:10.1007/s40544-013-0018-y.
[25] Tønder K. Hydrodynamic effects of tailored inlet roughnesses: extended theory. Tribol Int 2004;37:137–42. doi:10.1016/S0301-679X(03)00043-4.
[26] Greenwood JA, Morales-Espejel GE. The behaviour of transverse roughness in EHL contacts. Proc Inst Mech Eng Part J J Eng Tribol 1994;208:121–32. doi:10.1243/PIME.
[27] Morales-Espejel GE, Lugt PM, Van Kuilenburg J, Tripp JH. Effects of Surface Micro-Geometry on the Pressures and Internal Stresses of Pure Rolling EHL Contacts. Tribol Trans 2003;46:260–72. doi:10.1080/10402000308982625.
[28] Fowell M, Olver AV, Gosman AD, Spikes HA, Pegg IG. Entrainment and Inlet Suction: Two Mechanisms of Hydrodynamic Lubrication in Textured Bearings. J Tribol 2007;129:336–47. doi:10.1115/1.2540089.
[29] Olver AV, Fowell MT, Spikes HA, Pegg IG. “Inlet suction”, a load support mechanism in non-convergent, pocketed, hydrodynamic bearings. Proc Inst Mech Eng Part J J Eng Tribol 2006;220:105–8. doi:10.1243/13506501JET168.
[30] Varenberg M, Halperin G, Etsion I. Different aspects of the role of wear debris in fretting wear. Wear 2002;252:902–10.
[31] Vladescu SC, Medina S, Olver A V., Pegg IG, Reddyhoff T. Lubricant film thickness and friction force measurements in a laser surface textured reciprocating line contact simulating the piston ring-liner pairing. Tribol Int 2016;98:317–29. doi:10.1016/j.triboint.2016.02.026.
[32] Vlădescu S-C, Medina S, Olver AV, Pegg IG, Reddyhoff T. The Transient Friction Response of a Laser-Textured, Reciprocating Contact to the Entrainment of Individual Pockets. Tribol Lett 2016;62. doi:10.1007/s11249-016-0669-8.
[33] Vlădescu S-C, Olver AV, Pegg IG, Reddyhoff T. Combined friction and wear reduction in a reciprocating contact through laser surface texturing. Wear 2016;358-359:51–61. doi:10.1016/j.wear.2016.03.035.
[34] Medina S, Fowell MT, Vlădescu S-C, Reddyhoff T, Pegg I, Olver a. V., et al. Transient effects in lubricated textured bearings. Proc Inst Mech Eng Part J J Eng Tribol 2015;0:1–15. doi:10.1177/1350650115572448.
[35] Profito FJ, Vlădescu S-C, Reddyhoff T, Dini D. Transient experimental and modelling studies of laser-textured micro-grooved surfaces with a focus on piston-ring cylinder liner contacts. Tribol Int 2016:1–12. doi:10.1016/j.triboint.2016.12.003.
[36] Profito FJ, Vladescu S, Reddyhoff T, Dini D, Contacts TP. Experimental Validation of a Mixed-

Lubrication Regime Model for Textured Piston-Ring- Liner Contacts. Mater Perform Charact 2017;6. doi:10.1520/MPC20160019.
[37] Vlădescu S-C, Tufail K, Gangopadhyay A, Reddyhoff T. Optimisation of Pocket Geometry for Friction Reduction in Piston-Liner Contacts (IN PRESS). Tribol Trans 2017.
[38] Priest M, Dowson D, Taylor CM. Theoretical modelling of cavitation in piston ring lubrication. Proc Inst Mech Eng Part C J Mech Eng Sci 2000;214:435–46. doi:10.1243/0954406001523092.
[39] Gümbel LKR. Vergleich der Ergebrusse der rectinerischen Behandling des Lagerschmierangsproblem mitneueren Versuchsergebrussen. Monatsbl Berliner Bez Ver Dtsch Ing 1921:125–8.
[40] Swift HW. The stability of lubricating films in journal bearings. J Inst Civ Eng 1931;233:267–88.
[41] Stieber W. Das Schwimmlager. Ver Dtsch Ing 1933.
[42] Jakobson B, Floberg L. The finite journal bearing considering vaporization. Trans Chalmers Univ Technol Guthenberg, Sweden 1957;190:1–119.
[43] Olsson KO. Cavitation in Dynamically Loaded Bearings. Trans Chalmers Univ Technol Goteborg 1965:308.
[44] Floberg L. On journal bearing lubrication considering the tensile strength of the liquid lubricant. Vedmar, L Trans Mach Elem Div 1973:1–26.
[45] Floberg L. Cavitation boundary conditions with regard to the number of streamers and tensile strength of the liquid. Dowson, D, Godet, M, Taylor, CM Cavitation Relat Phenom Lubr Proc 1st Leeds– Lyon Symp Tribol 1974:31–6.
[46] Dowson D, Smith EH, Taylor CM. An experimental study of hydrodynamic film rupture in a steadily-loaded, non-conformal contact. Arch J Mech Eng Sci 1959-1982 (vols 1-23) 2006;22:71–8. doi:10.1243/JMES_JOUR_1980_022_018_02.
[47] Dowson D. Cavitation in lubricating films supporting small loads. Proc Institutional Mech Eng Conf Lubr Wear 1957:93–9.
[48] Etsion I, Ludwig LP. Observation of pressure variation in the cavitation region of submerged journal bearings. J Tribol 1982;104:157–63. doi:10.1115/1.3253174.
[49] Dellis P, Arcoumanis C. Cavitation development in the lubricant film of a reciprocating piston-ring assembly. Proc Inst Mech Eng Part J J Eng Tribol 2004;218:157–71. doi:10.1243/1350650041323340.
[50] Dhunput A, Teodorescu M, Arcoumanis C. Investigation of cavitation development in the lubricant film of piston-ring assemblies. J Phys Conf Ser 2007;85:012005. doi:10.1088/1742-6596/85/1/012005.
[51] Tang T, Morris N, Coupland J, Arevalo L. Cavitation Bubble Measurement in Tribological Contacts Using Digital Holographic Microscopy. Tribol Lett 2015;58. doi:10.1007/s11249-015-0488-3.
[52] Elrod HG. A Cavitation Algorithm. J Lubr Technol 1981.
[53] Chong WWF, Teodorescu M, Vaughan ND. Cavitation induced starvation for piston-ring/liner tribological conjunction. Tribol Int 2011;44:483–97. doi:10.1016/j.triboint.2010.12.008.
[54] Taylor R. Squeeze film lubrication in piston rings and reciprocating contacts. Proc Inst Mech Eng Part J J Eng Tribol 2015;0:1–12. doi:10.1177/1350650114564234.
[55] Papadopoulos P, Priest M, Rainforth WM. Investigation of fundamental wear mechanisms at the piston ring and cylinder wall interface in internal combustion engines. Proc Inst Mech Eng Part J J Eng Tribol 2007;221:333–43. doi:10.1243/13506501JET254.
[56] Priest M, Dowson D, Taylor CM. Predictive wear modelling of lubricated piston rings in a diesel engine. Wear 1999;231:89–101. doi:10.1016/S0043-1648(99)00125-8.
[57] Chiu YP. An Analysis and Prediction of Lubricant Film Starvation in Rolling Contact Systems. A S L E Trans 1974;17:22–35. doi:10.1080/05698197408981435.
[58] Costa HL, Hutchings IM. Hydrodynamic lubrication of textured steel surfaces under reciprocating sliding conditions. Tribol Int 2007;40:1227–38. doi:10.1016/j.triboint.2007.01.014.
[59] Pettersson U, Jacobson S. Friction and Wear Properties of Micro Textured DLC Coated Surfaces in Boundary Lubricated Sliding. Tribol Lett 2004;17:553–9. doi:10.1023/B:TRIL.0000044504.76164.4e.